Infection and Inflammation Imaging
Beyond FDG

Malte Kircher, MD, Constantin Lapa, MD*

KEYWORDS

• Inflammation • Infection • PET • Molecular imaging • Somatostatin receptors • CXCR4 • TSPO • NaF

KEY POINTS

- ^{18}F-FDG PET/CT is the standard of reference in nuclear imaging of infection and inflammation, but lacks specificity.
- Receptor-directed alternatives, such as tracers targeting somatostatin and chemokine receptors on proinflammatory cells have shown promising results in first clinical studies, especially in the setting of myocardial inflammation.
- Many further PET and SPECT probes directed at other specific inflammatory cell receptors, cell adhesion molecules, and proinflammatory cytokines and enzymes are currently being evaluated.

INTRODUCTION

Although inflammation is a crucial and beneficial process in the acute physiologic defense against pathogens, excessive, uncontrolled, or chronic inflammatory reactions can lead to numerous pathologic changes. These include rheumatic and autoimmune diseases, such as rheumatoid arthritis (RA) or vasculitis, as well as several cardiovascular and neurologic disorders.

Traditionally, 3-phase bone scintigraphy, ^{67}Ga-citrate scintigraphy, or white blood cell scintigraphy have been the mainstay of nuclear medicine imaging of inflammation and infection. Nowadays, PET imaging with the glucose analog 2-deoxy-2-[^{18}F]fluoro-D-glucose (^{18}F-FDG, FDG), which takes advantage of the increased glucose metabolism in proinflammatory target cells,[1] is the standard of reference for noninvasive visualization and monitoring of inflammatory processes. However, its nonspecificity and dependence on physiologic variables, such as glucose levels or renal function can limit its suitability in numerous clinical scenarios.

To overcome these shortcomings multiple other tracers have been developed. In this review we discuss nuclear imaging of inflammation using molecular probes beyond FDG and focusing on their cellular targets. Special emphasis is put on diagnostic tracers that have already been successfully applied clinically (**Table 1**).

TARGETING RECEPTORS ON THE CELL SURFACE

Somatostatin Receptor

Somatostatin receptors (SSTR), especially subtype $SSTR_{2A}$, are important diagnostic and therapeutic targets in oncology, with routine use in the management of neuroendocrine tumors and meningiomas. The G protein-coupled receptor can be targeted using synthetic somatostatin analogs, such as 1,4,7,10-tetraazacyclododecane-1,4,7,10-tetraacetic acid (DOTA)-D-Phe-Tyr3-octreotide (DOTA-TOC), DOTA-1-Nal(3)-octreotide (DOTA-NOC), or DOTA-D-Phe-Tyr3-octreotate (DOTA-TATE), which differ mainly in their affinity to the various receptor subtypes ($SSTR_{1-5}$). A particularly rich $SSTR_2$ expression is found on macrophages with numerous studies demonstrating promising results using SSTR-directed PET for detection of various

Department of Nuclear Medicine, University Hospital Augsburg, Stenglinstr. 2, Würzburg 86156, Germany
* Corresponding author.
E-mail address: Constantin.Lapa@uk-augsburg.de

PET Clin 15 (2020) 215–229
https://doi.org/10.1016/j.cpet.2019.11.004

Table 1
PET tracers for inflammation imaging

Target	Tracer	Features
Specific targeting of receptors/transporters/proteins		
Somatostatin receptor (SSTR)	^{68}Ga-DOTA-TOC ^{68}Ga-DOTA-NOC ^{68}Ga-DOTA-TATE	Overexpressed mainly on proinflammatory M1 macrophages. Useful particularly in imaging of cardiac inflammation due to specificity and lack of tracer uptake in healthy myocardium (FDG PET requires the use of dedicated patient preparation strategies to suppress the physiologic myocardial FDG uptake)
C-X-C motif chemokine receptor 4 (CXCR4)	^{68}Ga-Pentixafor	Expressed on a variety of proinflammatory immune cells, with a pronounced overexpression on macrophages and T cells
C-C motif chemokine receptor 2 (CCR2)	^{64}Cu-DOTA ECL1i ^{68}Ga-DOTA ECL1i	Mostly expressed on highly inflammatory monocytes, natural killer cells and T cells
$\alpha_v\beta_3$ integrin receptor	^{18}F-Galacto-RGD ^{68}Ga-PRGD2 ^{18}F-Fluciclatide	Mediates cell adhesion and plays an important role in angiogenesis, making it an interesting target in many different oncologic or inflammatory conditions, such as rheumatoid arthritis
Folate receptor (FR)	^{18}F-Fluoro-PEG-folate	Remarkably high expression on the cell surface of activated macrophages with highly restricted FR expression in normal tissues
Mannose receptor	^{18}F-Fluoro-D-mannose ^{68}Ga-NOTA-HAS ^{68}Ga-NOTA-anti-MMR nanobody	Mainly expressed by macrophages, immature dendritic cells, and liver sinusoidal endothelial cells
Translocator protein-18 kDa (TSPO)	^{11}C-PK11195 and 2nd and 3rd generation TSPO tracers, such as ^{18}F-GE180	Protein situated in the outer mitochondrial membrane; upregulated in activated macrophages, particularly in the brain (microglia). Promising target for neuroinflammation imaging.
Bacterial thymidine kinase	^{124}I-FIAU	Bacteria express a thymidine kinase (TK) that differs from the major human TK in its substrate specificity
Bacterial maltodextrin transporter	^{18}F-Maltohexaose	Bacteria-specific and not found in mammalian cells

(*continued on next page*)

Table 1
(*continued*)

Target	Tracer	Features
Unspecific visualization of inflammation		
Proliferation	^{11}C-Methionine	Marker of amino acid transport and protein synthesis, accumulates in inflammatory cells, including macrophages, T cells, and B cells
Proliferation	^{18}F-Fluorothymidine (FLT)	Generally considered a marker of tumor proliferation; able to visualize inflammation with different tracer distribution compared with FDG
Bone metabolism	^{18}F-Sodium flouride (NaF)	Used to assess bone metabolism and osteogenic activity; since NaF also localizes to developing microcalcifications, it can be used as a marker of calcification activity

inflammatory conditions, such as sarcoidosis, myocarditis, or atherosclerosis.

In a study with 20 patients with sarcoidosis, Nobashi and colleagues[2] demonstrated the superiority of ^{68}Ga-DOTA-TOC PET/computed tomography (CT) over ^{67}Ga-scintigraphy for identification of lymph node, uvea, and muscle lesions. Subsequent pilot studies used SSTR-directed PET to detect cardiac sarcoidosis (CS), with results corresponding closely to those of cardiac MR imaging,[3] and outperforming those of ^{18}F-FDG PET.[4] SSTR PET was likewise used to visualize myocardial inflammation in patients with pericarditis, myocarditis, and subacute myocardial infarction (AMI), again with excellent concordance to cardiac MR imaging.[5] Key advantages of SSTR-directed imaging of cardiac inflammation include specific targeting of proinflammatory M1 macrophages,[6] and lack of tracer uptake in healthy myocardium, a significant advantage over ^{18}F-FDG PET, which requires the use of dedicated patient preparation strategies to suppress the physiologic myocardial ^{18}F-FDG uptake.[7–9]

SSTR-directed PET imaging is furthermore capable of localizing inflammation in atherosclerosis. Although initial pilot studies established the general feasibility of this imaging approach in the larger arteries,[10,11] the prospective observational VISION trial, which included 42 patients with acute coronary syndrome and/or transient ischemic attack/stroke, revealed superior imaging characteristics of ^{68}Ga-DOTATATE versus ^{18}F-FDG PET in vessels as small as the coronary arteries[6] (**Fig. 1**). A substudy revealed that SSTR-directed PET can identify residual postinfarction myocardial inflammation both in recently infarcted myocardium (<3 months) as well as in old ischemic injuries,[12] and also found a strong correlation between bone marrow uptake and myocardial inflammation, which might indicate a potential for noninvasive evaluation of systemic inflammatory networks.[12] Finally, Schatka and colleagues[13] outlined the potential of SSTR-directed peptide receptor radionuclide therapy to alter inflammatory activity in atherosclerotic plaques, a potentially new theranostic approach to modulate plaque biology.

C-X-C Motif Chemokine Receptor 4

C-X-C motif chemokine receptor 4 (CXCR4) is expressed on a variety of proinflammatory immune cells, with a pronounced overexpression on macrophages and T cells. CXCR4-directed PET tracers, such as ^{68}Ga-Pentixafor provide the opportunity to visualize human CXCR4 expression in vivo, and insights from first pilot studies suggest that this approach can contribute to uncovering the highly sophisticated role of chemokines and their receptors in inflammatory processes.

Myocardial inflammation imaging after acute myocardial infarction

Pilot studies that investigated CXCR4-directed PET imaging in the highly inflammatory environment of AMI demonstrated high tracer uptake in the infarcted myocardium[14] (**Fig. 2**), which coincided with the presence of proinflammatory cells in the ischemic area.[15] A further investigation

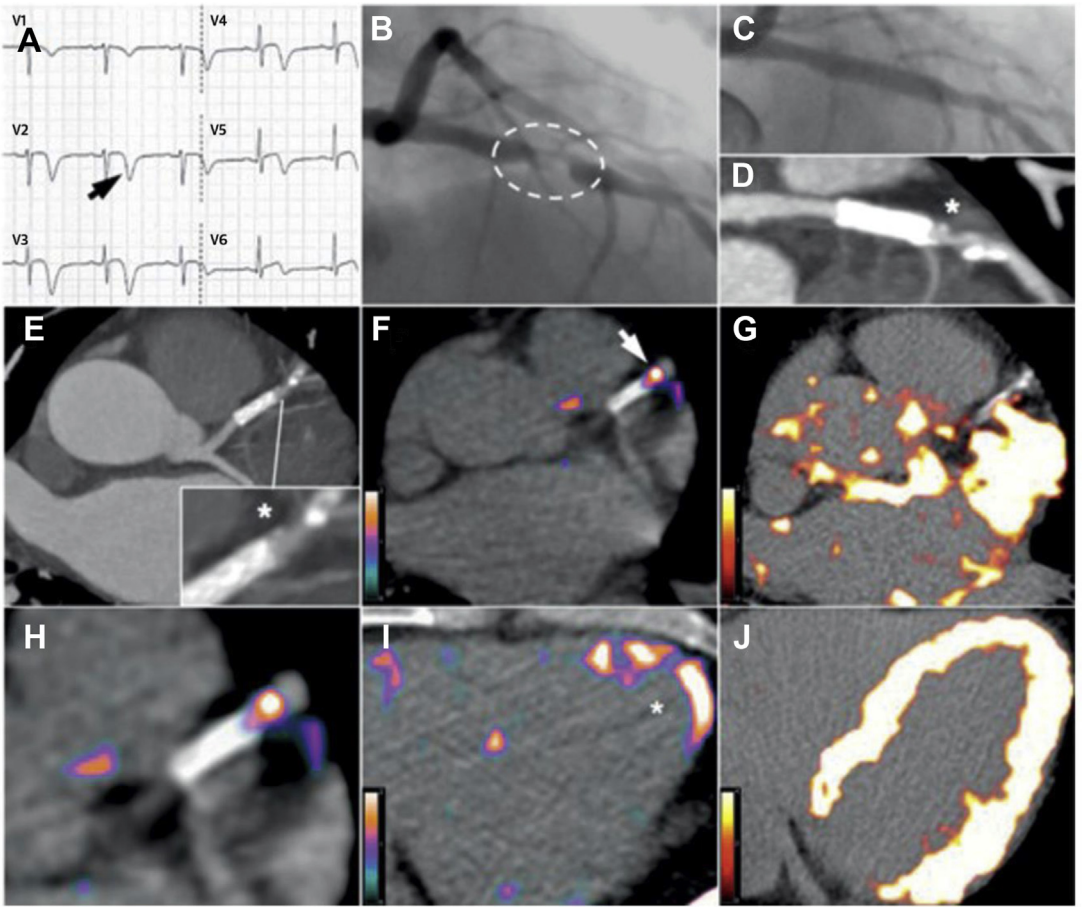

Fig. 1. Comparison between ^{68}Ga-DOTATATE and ^{18}F-FDG coronary PET inflammation imaging. Images from a 57-year-old man with acute coronary syndrome who presented with deep anterolateral T-wave inversion (*arrow*) on electrocardiogram (*A*) and serum troponin-I concentration increased at 4650 ng/L (NR: <17 ng/L). Culprit left anterior descending artery stenosis (dashed oval) was identified by X-ray angiography (*B*). After percutaneous coronary stenting (*C*), residual coronary plaque (*inset) with high-risk morphology (low attenuation and spotty calcification) is evident on CT angiography (*D*, *E*). ^{68}Ga-DOTATATE PET (*F*, *H*, *I*) clearly detected intense tracer accumulation in this atherosclerotic plaque/distal portion of the stented culprit lesion (*arrow*) and recently infarcted myocardium (*asterisk*). In contrast, in ^{18}F-FDG PET (*G*, *J*), myocardial spillover completely obscures the coronary arteries. CT, computed tomography; ^{18}F-FDG, fluorine-18-labeled fluorodeoxyglucose; ^{68}Ga-DOTATATE, gallium-68-labeled DOTATATE. (*From* Tarkin JM, Joshi FR, Evans NR, et al. Detection of Atherosclerotic Inflammation by (68)Ga-DOTATATE PET Compared to [(18)F]FDG PET Imaging. Journal of the American College of Cardiology. 2017;69(14):1774-1791; with permission.)

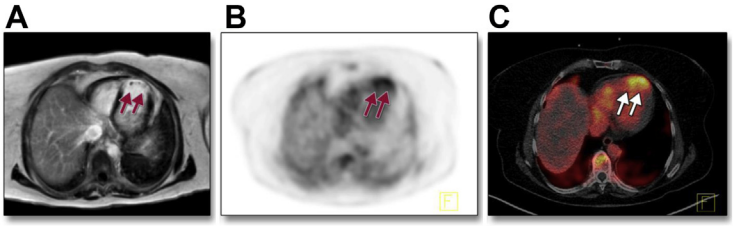

Fig. 2. Increased ^{68}Ga-Pentixafor uptake in acute myocardial infarction affecting the left anterior descending artery. Axial slices of both (*A*) contrast-enhanced multishot inversion recovery turbo field echo cardiac MR imaging and (*B*) CXCR4-PET, as well as (*C*) fused PET/computed tomography. Images reveal increased ^{68}Ga-Pentixafor uptake in the apex that consistently matches myocardial damage in CMR (*arrows*). (*From* Lapa C, Reiter T, Werner RA, et al. [(68)Ga]Pentixafor-PET/CT for Imaging of Chemokine Receptor 4 Expression After Myocardial Infarction. *JACC Cardiovascular imaging.* 2015;8(12):1466-1468; with permission.)

found a correlation between CXCR4 expression in the bone marrow and the severity of the systemic inflammatory response,[16] and showed that those patients with AMI who had initially high myocardial tracer uptake presented with less scar tissue in the infarcted area and a better functional outcome at follow-up.[16] However, the latter findings are in contradiction with results of a recent preclinical study that reported on beneficial effects of CXCR4 blockade by attenuated inflammatory gene expression via regulatory T cells.[17] More research to broaden our understanding of the spatial and temporal orchestration of CXCR4 expression in the different cell types involved in AMI is highly warranted.

C-X-C motif chemokine receptor 4-directed inflammation imaging in atherosclerosis

At present, a study of 72 patients with lymphoma showed that ^{68}Ga-Pentixafor PET/MRI is able to visualize inflammation within human carotid plaques, with histologic evidence for colocalization of CXCR4 and CD68 in inflamed atheromas and preatheromas.[18] These findings confirmed previous results of CXCR4 overexpression in macrophage-rich plaque regions in a rabbit model of atherosclerosis.[19] In addition, 2 independent studies demonstrated an association between cardiovascular risk factors and CXCR4 expression within atherosclerotic plaques on a per-patient basis, as visualized by ^{68}Ga-Pentixafor PET/CT.[20,21] Derlin and colleagues[22] investigated CXCR4 expression in the coronary arteries of 37 patients with AMI after stent-based reperfusion and found highest ^{68}Ga-Pentixafor uptake in the culprit lesions, which the authors ascribed to vessel wall inflammation and/or stent-induced injury. In another study in patients undergoing CXCR4-directed endoradiotherapy with ^{177}Lu-/^{90}Y-Pentixather for hematologic malignancy, Li and colleagues[23] were able to show an additional anti-inflammatory therapeutic effect on atherosclerotic plaques.

Whereas most of the PET signal is believed to originate from macrophages, the variety of different cell types expressing the chemokine receptor on their surface (T cells, B cells, and/or progenitor cells) adds complexity to the underlying biology and its clinical implications,[24] and the CXCR4 axis seems to exert both atheroprotective as well as atherogenic, proinflammatory effects.[25,26] This could explain results of a human carotid plaque study that showed CXCR4 overexpression in both stable and unstable atherosclerotic plaques, with the highest receptor expression found on macrophages and macrophage-derived foam cells.[27] Future studies to investigate CXCR4 biology in atherosclerosis and its clinical implications are highly warranted.

C-X-C motif chemokine receptor 4-directed imaging in infections

Noninvasive targeting of CXCR4 with PET/CT has also been used to image infectious diseases. In a pilot study of 29 patients with suspected chronic osteomyelitis, Bouter and colleagues[28] exploited the increased CXCR4 expression of T cells to successfully visualize inflammatory activity. In a separate study, the same group demonstrated superior diagnostic accuracy of ^{68}Ga-Pentixafor PET/CT for detection of chronic bone infections compared with the granulocyte-directed ^{99m}Tc-besilesomab and ^{99m}Tc-labeled white blood cells.[29] In addition, in an investigation of 13 patients with complicated urinary tract infections after kidney transplantation, infectious foci could successfully be detected by imaging leukocyte infiltration using ^{68}Ga-Pentixafor PET and MRI.[30]

C-C Motif Chemokine Receptor 2

C-C chemokine receptor type 2 (CCR 2; CD 192) is mostly expressed on monocytes, natural killer cells, and T lymphocytes,[31,32] and plays a crucial role in the homeostatic release of monocytes and macrophages from the bone marrow.[33] Interaction of CCR2 with its ligand CCL2 is essential to induce normal inflammatory monocyte migration (from the bone marrow) into peripheral tissues,[34] which is important in the defense against microbial infections. An imbalance in favor of highly inflammatory CCR2$^+$ macrophages and monocytes can, however, lead to serious pathologic changes and inflammatory conditions, such as atherosclerosis and RA.[35,36] Furthermore, it has been shown that, after AMI, CCR2$^+$ monocytes infiltrate the heart and differentiate into highly inflammatory CCR2$^+$ macrophages that ultimately contribute to postinfarction heart failure.[37]

With the development of the allosteric CCR2 ligand "extracellular loop 1 inverso" (ECL1i), noninvasive molecular imaging of CCR2 expression in vivo has become feasible,[38] as illustrated by the results of a pilot study in mice models of cardiac injury that showed accumulation of the new tracer in areas rich in CCR2$^+$ cells.[39] The authors also provided autoradiographic confirmation of specific tracer binding to human macrophages in heart failure specimens.[39] Another proof-of-concept could be provided in a mouse model of lung injury and in human tissues from subjects with chronic obstructive pulmonary disease.[40] PET using ^{64}Cu-labeled DOTA-ECL1i was able to noninvasively visualize CCR2$^+$ cells in both mouse

lungs (after LPS-induced injury) as well as in human lung disease tissue.[40]

Other Specific Targets

Alpha-v beta-3 receptor

The transmembrane receptor alpha-v beta-3 integrin ($\alpha_v\beta_3$) mediates cell adhesion and plays an important role in angiogenesis, making it an interesting target in many different oncologic or inflammatory conditions.[41,42] Radiopharmaceuticals containing an arginine-glycine-aspartic acid (RGD) sequence, such as ^{18}F-galacto-RGD, ^{68}Ga-PRGD2, and ^{18}F-fluciclatide bind the $\alpha_v\beta_3$ receptor with high affinity and enable noninvasive visualization of $\alpha_v\beta_3$ expression in vivo.[43]

In atherosclerosis, both macrophages and activated endothelial cells have been described to express high levels of the $\alpha_v\beta_3$ receptor.[44,45] Interestingly, the $\alpha_v\beta_3$ integrin may be directly involved in the degradation of the protective fibrous cap of atherosclerotic lesions, because it has been identified as a binding moiety that localizes matrix metalloproteinase 2 to the surface of invasive cells.[46,47] Therefore, $\alpha_v\beta_3$ expression might serve as a potential combined marker of both inflammation and angiogenesis in atherosclerotic lesions and thus as a noninvasive in vivo surrogate parameter of plaque vulnerability.[48] In a study in 10 patients with high-grade carotid artery stenosis, ^{18}F-galacto-RGD uptake significantly correlated with intraplaque $\alpha_v\beta_3$ expression and with results of autoradiography, and could be specifically blocked in in vitro competition experiments. Based on these results, the authors concluded that $\alpha_v\beta_3$-integrin-directed PET visualized several important features of plaque stability that might potentially be advantageous over ^{18}F-FDG.[49] Another study of 21 patients with AMI using the RGD-containing tracer ^{18}F-fluciclatide showed increased tracer uptake in the infarcted area, which the authors attributed to sites of cardiac repair, due to an association between tracer uptake and functional recovery at follow-up.[50] This confirmed results of previous studies with other $\alpha_v\beta_3$-directed PET tracers in a rat model of AMI,[51] and in patients with AMI/stroke.[52]

Apart from cardiovascular imaging, $\alpha_v\beta_3$-directed PET has been used to image conditions associated with angiogenesis, highlighted by a prospectively designed head-to-head comparison between ^{68}Ga-PRGD2 and ^{18}F-FDG PET/CT in 20 patients with untreated RA.[53] The authors demonstrated the superiority of ^{68}Ga-PRGD2 over ^{18}F-FDG for detection and evaluation of severity of active RA lesions and provided histologic confirmation of increased $\alpha_v\beta_3$ expression on neo-endothelial cells of the affected synovia.[53]

Mitochondrial translocator protein

The 18-kDa mitochondrial translocator protein (TSPO) is a 5-transmembrane domain protein situated in the outer mitochondrial membrane and is widely distributed in most peripheral organs, including kidneys, nasal epithelium, adrenal glands, lungs, and heart.[54] In contrast, due to minimal expression in resting microglial cells, it has been found to be a promising target for neuroinflammation imaging.[55] Because TSPO is also upregulated in activated macrophages, its use might be extended to the visualization of non-neurologic, peripheral inflammatory processes as well as the characterization of systemic inflammatory responses, for example, the heart-brain axis after myocardial infarction.

In a series of trials of patients with RA, TSPO-directed PET was able to detect subclinical synovitis via imaging of activated macrophages, even when MRI was inconspicuous.[56–59] In studies in the setting of atherosclerosis and vascular inflammation in patients with systemic inflammatory disorders, the selective TSPO ligand ^{11}C-PK11195 was able to visualize activated macrophages in the vessel wall and improve cerebrovascular risk stratification.[60–62] Of note, TSPO PET detected inflammatory activity even in asymptomatic patients and might therefore prove a useful tool for very early disease detection. However, some limitations of TSPO PET tracers for the detection of peripheral inflammatory conditions, such as its multicellular receptor expression profile, the presence of radiolabeled metabolites and an interindividual variability of tracer binding affinity due to TSPO polymorphisms have to be taken into account.[63] Beyond these drawbacks, strengths of TSPO-directed PET imaging are the ability to visualize both central and peripheral inflammatory networks and the interplay between activated microglia and macrophages, as highlighted in a recent study by Thackeray and colleagues.[64] In a mouse model of AMI the authors revealed that, in addition to the inflammatory response in the infarcted myocardium, there was an interaction between systemic inflammatory networks and neuronal inflammation via activated microglia (**Fig. 3**). These results could be corroborated in 3 patients after AMI, thus highlighting the systemic interaction between heart and brain after cardiac ischemia. A pilot study in patients with controlled HIV infection also hinted at the suitability of TSPO PET to depict concomitant neuroinflammation.[65]

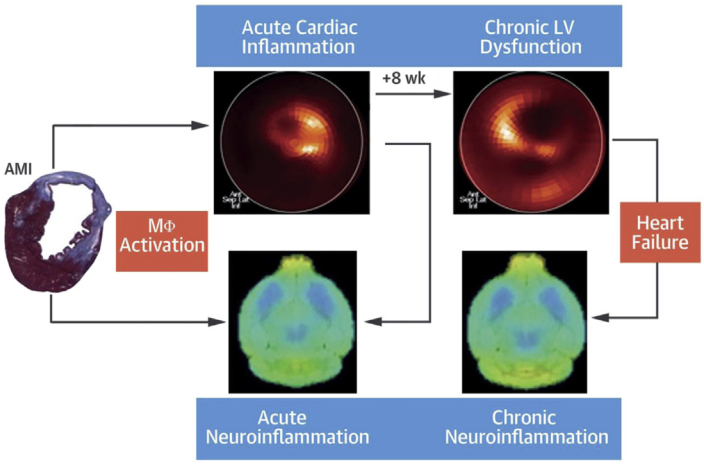

Fig. 3. Serial imaging demonstrating concurrent increase of TSPO in the heart and brain after acute MI and in chronic heart failure. Distribution of the mitochondrial translocator protein (TSPO) ligand ^{18}F-GE180 denotes inflammation in the heart and brain after acute myocardial infarction. Perfusion-corrected ^{18}F-GE180 polar map shows increased TSPO expression in the anterolateral infarct territory at 1 week post-MI, associated with increased TSPO and neuroinflammation. After 8 weeks and the development of heart failure, TSPO is increased in the remote myocardium with recurrent neuroinflammation proportional to the decline in cardiac function. AMI, acute myocardial infarction; MΦ, macrophage. (*From* Thackeray JT, Hupe HC, Wang Y, et al. Myocardial Inflammation Predicts Remodeling and Neuroinflammation After Myocardial Infarction. Journal of the American College of Cardiology. 2018;71(3):263-275; with permission.)

Folate receptor

Folate receptor beta (FR-β) is a glycosylphosphatidylinositol-anchored protein that binds the vitamin folic acid with high affinity and internalizes it via endocytosis.[66] Except for an overexpression on proximal tubule cells in the kidneys, FR prevalence is limited in normal tissues. However, a remarkably high FR expression on the surface of activated macrophages has been described,[67] and FRs have been targeted to study inflammatory conditions, such as RA. An example is a study by Gent and colleagues[68] in a rat model of RA that demonstrated superiority of ^{18}F-fluoro-PEG-folate over the mitochondrial translocator protein PET tracer PK11195 for detection of RA. In another study, FR-targeted PET was able to identify affected joints in patients with RA and provided histologic proof from synovial tissue samples.[69] Numerous other preclinical studies are currently evaluating the potential of targeting the FR-β for diagnosis and treatment of inflammatory diseases (mainly RA).[70,71]

Mannose receptor

The mannose receptor (CD206) is mainly expressed by macrophages, immature dendritic cells, and liver sinusoidal endothelial cells,[72] and several preclinical studies have already evaluated the possibility of targeting it for inflammation imaging. For example, ^{18}F-fluoro-D-mannose PET/CT was used in a rabbit model to identify inflammation within atherosclerotic plaques,[73] whereas ^{68}Ga-NOTA-mannosylated human serum albumin (MSA) PET was successfully utilized in different animal models for detection of inflammation in atherosclerotic plaques and myocarditis, respectively.[74,75] Recently, a study in apoE-knock out mice demonstrated feasibility of atherosclerotic plaque imaging by visualization of (M2a) macrophages using a ^{68}Ga-labeled anti-MR-nanobody.[76]

Thymidine kinase

Bacteria express a thymidine kinase (TK) that differs from the major human TK in its substrate specificity. This was exploited by Diaz and colleagues[77] who used ^{124}I-labeled 1-(2′-deoxy-2′-fluoro-b-D-arabinofuranosyl)-5-iodouracil (FIAU), a substrate of the bacteria TK, to detect musculoskeletal infections in a pilot study with 8 patients. But despite these promising results, the whole-body distribution with significant uptake in liver, kidneys, muscles, and to a lesser extent in several other organs, potentially due to the presence of a mitochondrial enzyme resembling the bacterial TK, raised concerns about the general applicability of the tracer. These concerns were reaffirmed in a study on ^{124}I-FIAU PET for detection of prosthetic joint infections that revealed low specificity and sensitivity of the tracer.[78]

Maltodextrin transporter

The bacteria-specific maltodextrin transporter is not found in mammalian cells and can be targeted with ^{18}F-labeled maltohexaose (^{18}F-MH). Ning and colleagues[79] showed in rats that ^{18}F-MH PET can identify early stage infections consisting of as few as 10^5 colony-forming units of *E. coli*. In a recent investigation using a model of *Staphylococcus aureus*-mediated infections associated with implanted cardiac devices, ^{18}F-MH but not ^{18}F-FDG PET was able to distinguish infection from

noninfectious inflammation.[80] Thus, this new imaging probe holds great potential for the translation of bacterial imaging in humans.

Other targeted tracers

Numerous other imaging probes have been investigated that cannot be extensively covered in this review, including receptor-directed tracers that target immune cells, such as T lymphocytes (CD3 and CD4) and B lymphocytes (CD20), or granulocytes (BW250/183),[81] as well as tracers for specific noninvasive imaging of bacterial infections. For a comprehensive overview over the current literature and most promising candidates for infection-specific PET imaging of bacteria, please refer to the review by Auletta and colleagues.[82]

TARGETING CELL PROLIFERATION AND CELL METABOLISM

As an alternative to receptor-directed imaging, tracers targeting increased inflammatory cell metabolism have been evaluated. Although these tracers are obviously not inflammation specific, they may offer advantages over ^{18}F-FDG in certain scenarios, for example, for the assessment of inflammatory heart processes, such as myocarditis or sarcoidosis, due to the absence of physiologic uptake in the healthy myocardium.

Methionine

The radiolabeled amino acid L-[methyl-^{11}C]methionine (^{11}C-methionine) as a marker of amino acid transport and protein synthesis is predominantly used in oncology, particularly for the imaging of brain tumors and multiple myeloma.[83–87] However, methionine uptake is also increased in monocytes and macrophages that migrate to sites of inflammatory activity.[88,89] In vitro binding experiments using isolated inflammatory cells confirmed that ^{14}C-methionine accumulates in inflammatory cells, including macrophages, T cells, and B cells,[90] suggesting the applicability of ^{11}C-methionine PET for detection of inflammatory lesions, especially in the setting after acute ischemia. In a pilot study of 9 patients with AMI, Morooka and colleagues[91] demonstrated increased myocardial ^{11}C-methionine uptake in the infarct area, with reduced or no uptake in ^{18}F-FDG PET and ^{201}Tl perfusion SPECT, respectively. Thackeray and colleagues[92] confirmed these results by tracing ^{11}C-methionine accumulation in the infarcted area back to inflammatory M1 macrophages using a mouse model and 1 human patient. Increased uptake of ^{11}C-methionine was also found in inflammatory lesions of a rat model with induced autoimmune inflammatory myocarditis.[93]

Fluorothymidine

3′-Deoxy-3′-^{18}F-fluorothymidine (FLT) has been mostly evaluated in the oncologic setting as a marker of tumor proliferation. FLT is transported into the cell by nucleoside transporters, phosphorylated by thymidine kinase 1 (which is particularly active between the late G1 and early G2 phase of the cell cycle), and subsequently trapped within the cell.[94] Thus, FLT also holds promise as a tracer to image inflammation by depicting cell proliferation.

In a mouse model of experimental RA, FLT PET/CT revealed enhanced tracer uptake in inflamed ankles as early as 1 day after arthritis induction. Imaging findings correlated strongly with immunohistochemical Ki67 staining and was therefore considered a promising tool for the in vivo assessment of arthritic joint inflammation.[95] Clinical experience with FLT is currently growing for sarcoidosis. Norikane and colleagues[96] studied 20 patients with sarcoidosis, who underwent both FLT and FDG PET/CT. FLT was able to identify CS and extracardiac lesions, but tracer uptake was lower as compared with FDG. Recently, a pilot study reported on an equally excellent performance of FLT PET in the detection of CS as compared with FDG. Interestingly, the distribution pattern of the 2 tracers in the myocardium differed, suggesting a distinct pathophysiological source of the respective signal.[97] Further research including of the value of FLT PET as a biomarker for CS is warranted.

Sodium Fluoride

PET imaging with sodium ^{18}F-fluoride (NaF) has been extensively used to assess bone metabolism and osteogenic activity.[98] Because NaF also localizes to developing microcalcifications, it can be used as a marker of calcification activity and has been investigated in a range of cardiovascular disorders including aortic stenosis or atherosclerosis, and other inflammatory conditions, such as RA. In an experimental mouse model of RA, NaF PET identified sites of enhanced pathologic bone metabolism in diseased joints. In addition, the PET signal significantly correlated with the degree of bone destruction.[99] A study comparing NaF and FDG PET in 12 patients with RA found a similar distribution pattern of both tracers, with NaF PET being able to successfully identify RA-affected joints.[100]

Many studies have been performed for the evaluation of NaF PET for the characterization of vascular wall microcalcifications and could confirm the feasibility of this approach for large (aorta), carotid, and even coronary arteries.[101–104]

We refer to recent reviews for more detailed information.[105,106] Of note, the NaF PET signal did not colocalize with morphologic calcification (as detected by CT) or vessel wall inflammation (as detected by FDG PET) in a significant number of cases, suggesting that all modalities target distinct biological processes and stages in atherosclerosis. Beyond mere identification of sites of active calcification, NaF PET might serve as a noninvasive biomarker of increased cardiovascular risk. Among neurologically asymptomatic oncology patients undergoing NaF PET/CT, tracer accumulation in the common carotid arteries was correlated with cardiovascular risk factors and carotid calcified plaque burden.[101] In patients after recent transient ischemic attack or minor ischemic stroke, NaF PET was equally useful to highlight culprit and high-risk carotid plaques.[107] The predictive value of NaF PET could be confirmed for coronary atherosclerotic plaques (with NaF, but not FDG PET) and thoracic aorta calcification (with patients exhibiting high NaF uptake being prone to a 3.7 times higher cardiovascular disease risk based on the Framingham risk score)[108] as well as for symptomatic peripheral arterial disease (with NaF uptake demonstrating excellent discrimination in predicting 1-year restenosis after lower limb percutaneous transluminal angioplasty).[109] In contrast to these encouraging results, the suitability of NaF PET to detect active CS needs to be determined.[110]

OTHER TRACERS

Numerous PET tracers have been developed and are being evaluated for the purpose of infection and inflammation imaging, including tracers targeting most antibiotics, adhesion molecules, such as members of the integrin and selectin family, the immunoglobulin superfamily, or cytokines and enzymes, for example, matrix metalloproteinase or tumor necrosis factor alpha.[81]

Vascular adhesion protein-1 is a glycoprotein on endothelial cells and is involved in the transfer of leukocytes from blood to tissues on inflammation.[111] Several promising radiolabeled antibodies and peptides have been assessed.[111–115]

Selectins are single-chain transmembrane glycoproteins and are classified into 3 subtypes (L-, E−, and P-selectins) depending on the cell type on which they originate.[116] P-selectin is located in the α-granules of platelets and is expressed by activated endothelia.[117] Thus, it can be used as a target for imaging atherosclerosis, and radiolabeled probes for imaging P-selectin including Fucoidan have been assessed in preclinical models.[118–120]

The P2X7 receptor, a member of the purinergic family of receptors, is an adenosine triphosphate-gated ion channel expressed predominantly on macrophages and monocytes in the periphery and on microglia and astrocytes in the central nervous system. Because of its widespread involvement in inflammatory diseases as a key regulatory element of the inflammasome complex, with initiation and sustenance of the inflammatory cascade, it has attracted some attention and various SPECT and PET tracers have been evaluated.[121–126] In a recent inflammation versus tumor model in mice, the ^{18}F-labeled PsX7 tracer ^{18}F-PTTP (5-1-pyrimidin-2-yl-4,5,6,7-tetrahydro-1H-[1,2,3]triazolo[4,5-c]pyridin) showed promise to differentiate inflammation from malignancy.[127]

Another promising target is fibroblast activation protein (FAP), a 170-kDa transmembrane glycoprotein that has dipeptidyl peptidase and endopeptidase activity and shows high upregulation in epithelial carcinoma and sites of tissue remodeling, including fibrosis and arthritis.[128] Several radiolabeled antibodies have been used to target and image FAP expression in malignant and inflamed tissues, particularly in RA.[129–132] Recently, PET tracers based on small-molecule enzyme inhibitors have become clinically available.[133,134]

Various studies have looked at nanoparticles that are internalized by macrophages through phagocytosis.[135] Keliher and colleagues[136] were able to visualize cardiovascular inflammation in mice and rabbits using an ^{18}F-labeled, modified polyglucose nanoparticle called Macroflor with high avidity for macrophages.

SUMMARY

^{18}F-FDG PET/CT is by far the most established tracer in nuclear medicine infection and inflammation imaging and has proven its value in various clinical settings including fever of unknown origin,[137] endocarditis,[138] or sarcoidosis.[139] However, the glucose analog FDG is taken up by almost any metabolically active tissue, limiting its specificity for detecting inflammatory cells. In fact, in the setting of atherosclerosis, microautoradiography studies of aortic sections of ApoE$^{-/-}$ mice have shown that ^{14}C-FDG uptake into atherosclerotic plaques correlates poorly with fat content and selective macrophage staining with anti-CD68.[140] In addition, persistent vascular FDG uptake in patients with clinically controlled arteritis could not always reliably identify the subjects at risk to relapse,[141] thus raising concerns about the utility of FDG PET in the

follow-up of vasculitis and rendering its use to monitor disease activity controversial.[142]

Moreover, physiologic tracer uptake can severely impair the diagnostic performance in some scenarios (e.g. CS) requiring dedicated patient preparation.[143]

To overcome these limitations, many—potentially more specific—alternatives for noninvasive infection and inflammation imaging have been explored. At present, the clinically best established compounds target SSTRs on the cell surface of M1 macrophages, with a growing body of evidence suggesting the superiority of the SSTR-directed approach, particularly in coronary arteries.[6]

Many other monocyte-/macrophage-targeting tracers, such as mannose receptor, CCR2, or P2X7, have demonstrated encouraging preclinical results but need to be further assessed in clinical trials.

In atherosclerosis, detection of active calcification by means of NaF PET/CT is gaining growing attention.

Another clinically established option includes imaging of CXCR4 that holds potential for the detection of systemic inflammatory networks and could be especially used to monitor receptor-directed therapies, for example, after AMI. However, given the high abundance of different CXCR4-expressing cell types, further research investigating the different sources of the PET signal in different conditions is still needed until firm conclusions on the value of chemokine receptor-directed PET imaging can be drawn. The same holds true for most other promising compounds that have shown encouraging results in specific scenarios but are to be fully validated until their routine use instead of or complimentary to ^{18}F-FDG can be recommended.

CONFLICTS OF INTERESTS

The authors declare no conflicts of interest.

REFERENCES

1. Meller J, Sahlmann CO, Scheel AK. ^{18}F-FDG PET and PET/CT in fever of unknown origin. J Nucl Med 2007;48(1):35–45.
2. Nobashi T, Nakamoto Y, Kubo T, et al. The utility of PET/CT with (68)Ga-DOTATOC in sarcoidosis: comparison with (67)Ga-scintigraphy. Ann Nucl Med 2016;30(8):544–52.
3. Lapa C, Reiter T, Kircher M, et al. Somatostatin receptor based PET/CT in patients with the suspicion of cardiac sarcoidosis: an initial comparison to cardiac MRI. Oncotarget 2016;7(47):77807–14.
4. Gormsen LC, Haraldsen A, Kramer S, et al. A dual tracer (68)Ga-DOTANOC PET/CT and (18)F-FDG PET/CT pilot study for detection of cardiac sarcoidosis. EJNMMI Res 2016;6(1):52.
5. Lapa C, Reiter T, Li X, et al. Imaging of myocardial inflammation with somatostatin receptor based PET/CT—a comparison to cardiac MRI. Int J Cardiol 2015;194:44–9.
6. Tarkin JM, Joshi FR, Evans NR, et al. Detection of atherosclerotic inflammation by (68)Ga-DOTATATE PET compared to [(18)F]FDG PET imaging. J Am Coll Cardiol 2017;69(14):1774–91.
7. Harisankar CN, Mittal BR, Agrawal KL, et al. Utility of high fat and low carbohydrate diet in suppressing myocardial FDG uptake. J Nucl Cardiol 2011;18(5):926–36.
8. Williams G, Kolodny GM. Suppression of myocardial 18F-FDG uptake by preparing patients with a high-fat, low-carbohydrate diet. AJR Am J Roentgenol 2008;190(2):W151–6.
9. Ishimaru S, Tsujino I, Takei T, et al. Focal uptake on ^{18}F-fluoro-2-deoxyglucose positron emission tomography images indicates cardiac involvement of sarcoidosis. Eur Heart J 2005;26(15):1538–43.
10. Li X, Bauer W, Kreissl MC, et al. Specific somatostatin receptor II expression in arterial plaque: (68)Ga-DOTATATE autoradiographic, immunohistochemical and flow cytometric studies in apoE-deficient mice. Atherosclerosis 2013;230(1):33–9.
11. Li X, Samnick S, Lapa C, et al. ^{68}Ga-DOTATATE PET/CT for the detection of inflammation of large arteries: correlation with ^{18}F-FDG, calcium burden and risk factors. EJNMMI Res 2012;2(1):52.
12. Tarkin JM, Calcagno C, Dweck MR, et al. 68)Ga-DOTATATE PET identifies residual myocardial inflammation and bone marrow activation after myocardial infarction. J Am Coll Cardiol 2019;73(19):2489–91.
13. Schatka I, Wollenweber T, Haense C, et al. Peptide receptor-targeted radionuclide therapy alters inflammation in atherosclerotic plaques. J Am Coll Cardiol 2013;62(24):2344–5.
14. Lapa C, Reiter T, Werner RA, et al. [(68)Ga]Pentixafor-PET/CT for imaging of chemokine receptor 4 expression after myocardial infarction. JACC Cardiovasc Imaging 2015;8(12):1466–8.
15. Thackeray JT, Derlin T, Haghikia A, et al. Molecular imaging of the chemokine receptor CXCR4 after acute myocardial infarction. JACC Cardiovasc Imaging 2015;8(12):1417–26.
16. Reiter T, Kircher M, Schirbel A, et al. Imaging of C-X-C motif chemokine receptor CXCR4 expression after myocardial infarction with [(68)Ga]Pentixafor-PET/CT in correlation with cardiac MRI. JACC Cardiovasc Imaging 2018;11(10):1541–3.
17. Wang Y, Dembowsky K, Chevalier E, et al. C-X-C motif chemokine receptor 4 blockade promotes

tissue repair after myocardial infarction by enhancing regulatory T cell mobilization and immune-regulatory function. Circulation 2019; 139(15):1798–812.
18. Li X, Yu W, Wollenweber T, et al. [(68)Ga]Pentixafor PET/MR imaging of chemokine receptor 4 expression in the human carotid artery. Eur J Nucl Med Mol Imaging 2019;46(8):1616–25.
19. Hyafil F, Pelisek J, Laitinen I, et al. Imaging the cytokine receptor CXCR4 in atherosclerotic plaques with the radiotracer (68)Ga-pentixafor for PET. J Nucl Med 2017;58(3):499–506.
20. Li X, Heber D, Leike T, et al. [68Ga]Pentixafor-PET/MRI for the detection of Chemokine receptor 4 expression in atherosclerotic plaques. Eur J Nucl Med Mol Imaging 2018;45(4):558–66.
21. Weiberg D, Thackeray JT, Daum G, et al. Clinical molecular imaging of chemokine receptor CXCR4 expression in atherosclerotic plaque using (68) Ga-pentixafor PET: correlation with cardiovascular risk factors and calcified plaque burden. J Nucl Med 2018;59(2):266–72.
22. Derlin T, Sedding DG, Dutzmann J, et al. Imaging of chemokine receptor CXCR4 expression in culprit and nonculprit coronary atherosclerotic plaque using motion-corrected [(68)Ga]pentixafor PET/CT. Eur J Nucl Med Mol Imaging 2018; 45(11):1934–44.
23. Li X, Kemmer L, Zhang X, et al. Anti-inflammatory effects on atherosclerotic lesions induced by CXCR4-directed endoradiotherapy. J Am Coll Cardiol 2018;72(1):122–3.
24. Pawig L, Klasen C, Weber C, et al. Diversity and inter-connections in the CXCR4 chemokine receptor/ligand family: molecular perspectives. Front Immunol 2015;6:429.
25. van der Vorst EP, Doring Y, Weber C. MIF and CXCL12 in cardiovascular diseases: functional differences and similarities. Front Immunol 2015;6: 373.
26. Doring Y, Pawig L, Weber C, et al. The CXCL12/CXCR4 chemokine ligand/receptor axis in cardiovascular disease. Front Physiol 2014;5:212.
27. Merckelbach S, van der Vorst EPC, Kallmayer M, et al. Expression and cellular localization of CXCR4 and CXCL12 in human carotid atherosclerotic plaques. Thromb Haemost 2018;118(1): 195–206.
28. Bouter Y, Meller B, Sahlmann CO, et al. Immunohistochemical detection of chemokine receptor 4 expression in chronic osteomyelitis confirms specific uptake in ^{68}Ga-Pentixafor-PET/CT. Nuklearmedizin 2018;57(5):198–203.
29. Bouter C, Meller B, Sahlmann CO, et al. 68)Ga-Pentixafor PET/CT imaging of chemokine receptor CXCR4 in chronic infection of the bone: first insights. J Nucl Med 2018;59(2):320–6.
30. Derlin T, Gueler F, Brasen JH, et al. Integrating MRI and chemokine receptor CXCR4-targeted PET for detection of leukocyte infiltration in complicated urinary tract infections after kidney transplantation. J Nucl Med 2017;58(11):1831–7.
31. Charo IF, Ransohoff RM. The many roles of chemokines and chemokine receptors in inflammation. N Engl J Med 2006;354(6):610–21.
32. Tomankova T, Kriegova E, Liu M. Chemokine receptors and their therapeutic opportunities in diseased lung: far beyond leukocyte trafficking. Am J Physiol Lung Cell Mol Physiol 2015;308(7): L603–18.
33. Shi C, Pamer EG. Monocyte recruitment during infection and inflammation. Nat Rev Immunol 2011;11(11):762–74.
34. Griffith JW, Sokol CL, Luster AD. Chemokines and chemokine receptors: positioning cells for host defense and immunity. Annu Rev Immunol 2014;32: 659–702.
35. Raghu H, Lepus CM, Wang Q, et al. CCL2/CCR2, but not CCL5/CCR5, mediates monocyte recruitment, inflammation and cartilage destruction in osteoarthritis. Ann Rheum Dis 2017;76(5):914–22.
36. Verweij SL, Duivenvoorden R, Stiekema LCA, et al. CCR2 expression on circulating monocytes is associated with arterial wall inflammation assessed by ^{18}F-FDG PET/CT in patients at risk for cardiovascular disease. Cardiovasc Res 2018;114(3): 468–75.
37. Bajpai G, Schneider C, Wong N, et al. The human heart contains distinct macrophage subsets with divergent origins and functions. Nat Med 2018; 24(8):1234–45.
38. Auvynet C, Baudesson de Chanville C, Hermand P, et al. ECL1i, d(LGTFLKC), a novel, small peptide that specifically inhibits CCL2-dependent migration. FASEB J 2016;30(6):2370–81.
39. Heo GS, Kopecky B, Sultan D, et al. Molecular imaging visualizes recruitment of inflammatory monocytes and macrophages to the injured heart. Circ Res 2019;124(6):881–90.
40. Liu Y, Gunsten SP, Sultan DH, et al. PET-based imaging of chemokine receptor 2 in experimental and disease-related lung inflammation. Radiology 2017;283(3):758–68.
41. Brooks PC, Clark RA, Cheresh DA. Requirement of vascular integrin alpha v beta 3 for angiogenesis. Science 1994;264(5158):569–71.
42. Brooks PC, Montgomery AM, Rosenfeld M, et al. Integrin alpha v beta 3 antagonists promote tumor regression by inducing apoptosis of angiogenic blood vessels. Cell 1994;79(7):1157–64.
43. Dijkgraaf I, Beer AJ, Wester HJ. Application of RGD-containing peptides as imaging probes for alphavbeta3 expression. Front Biosci (Landmark Ed) 2009;14:887–99.

44. Hoshiga M, Alpers CE, Smith LL, et al. Alpha-v beta-3 integrin expression in normal and atherosclerotic artery. Circ Res 1995;77(6):1129–35.
45. Antonov AS, Kolodgie FD, Munn DH, et al. Regulation of macrophage foam cell formation by alphaV-beta3 integrin: potential role in human atherosclerosis. Am J Pathol 2004;165(1):247–58.
46. van Hinsbergh VW, Engelse MA, Quax PH. Pericellular proteases in angiogenesis and vasculogenesis. Arterioscler Thromb Vasc Biol 2006;26(4):716–28.
47. Brooks PC, Stromblad S, Sanders LC, et al. Localization of matrix metalloproteinase MMP-2 to the surface of invasive cells by interaction with integrin alpha v beta 3. Cell 1996;85(5):683–93.
48. Razavian M, Marfatia R, Mongue-Din H, et al. Integrin-targeted imaging of inflammation in vascular remodeling. Arterioscler Thromb Vasc Biol 2011;31(12):2820–6.
49. Beer AJ, Pelisek J, Heider P, et al. PET/CT imaging of integrin alphavbeta3 expression in human carotid atherosclerosis. JACC Cardiovasc Imaging 2014;7(2):178–87.
50. Jenkins WS, Vesey AT, Stirrat C, et al. Cardiac alphaVbeta3 integrin expression following acute myocardial infarction in humans. Heart 2017;103(8):607–15.
51. Higuchi T, Bengel FM, Seidl S, et al. Assessment of alphavbeta3 integrin expression after myocardial infarction by positron emission tomography. Cardiovasc Res 2008;78(2):395–403.
52. Sun Y, Zeng Y, Zhu Y, et al. Application of (68)Ga-PRGD2 PET/CT for alphavbeta3-integrin imaging of myocardial infarction and stroke. Theranostics 2014;4(8):778–86.
53. Zhu Z, Yin Y, Zheng K, et al. Evaluation of synovial angiogenesis in patients with rheumatoid arthritis using (6)(8)Ga-PRGD2 PET/CT: a prospective proof-of-concept cohort study. Ann Rheum Dis 2014;73(6):1269–72.
54. Banati RB. Visualising microglial activation in vivo. Glia 2002;40(2):206–17.
55. Dupont AC, Largeau B, Santiago Ribeiro MJ, et al. Translocator protein-18 kDa (TSPO) positron emission tomography (PET) imaging and its clinical impact in neurodegenerative diseases. Int J Mol Sci 2017;18(4) [pii:E785].
56. van der Laken CJ, Elzinga EH, Kropholler MA, et al. Noninvasive imaging of macrophages in rheumatoid synovitis using 11C-(R)-PK11195 and positron emission tomography. Arthritis Rheum 2008;58(11):3350–5.
57. Gent YY, Voskuyl AE, Kloet RW, et al. Macrophage positron emission tomography imaging as a biomarker for preclinical rheumatoid arthritis: findings of a prospective pilot study. Arthritis Rheum 2012;64(1):62–6.
58. Gent YY, Ter Wee MM, Voskuyl AE, et al. Subclinical synovitis detected by macrophage PET, but not MRI, is related to short-term flare of clinical disease activity in early RA patients: an exploratory study. Arthritis Res Ther 2015;17:266.
59. Gent YY, Ahmadi N, Voskuyl AE, et al. Detection of subclinical synovitis with macrophage targeting and positron emission tomography in patients with rheumatoid arthritis without clinical arthritis. J Rheumatol 2014;41(11):2145–52.
60. Pugliese F, Gaemperli O, Kinderlerer AR, et al. Imaging of vascular inflammation with [^{11}C]-PK11195 and positron emission tomography/computed tomography angiography. J Am Coll Cardiol 2010;56(8):653–61.
61. Lamare F, Hinz R, Gaemperli O, et al. Detection and quantification of large-vessel inflammation with ^{11}C-(R)-PK11195 PET/CT. J Nucl Med 2011;52(1):33–9.
62. Gaemperli O, Shalhoub J, Owen DR, et al. Imaging intraplaque inflammation in carotid atherosclerosis with 11C-PK11195 positron emission tomography/computed tomography. Eur Heart J 2012;33(15):1902–10.
63. Owen DR, Yeo AJ, Gunn RN, et al. An 18-kDa translocator protein (TSPO) polymorphism explains differences in binding affinity of the PET radioligand PBR28. J Cereb Blood flow Metab 2012;32(1):1–5.
64. Thackeray JT, Hupe HC, Wang Y, et al. Myocardial inflammation predicts remodeling and neuroinflammation after myocardial infarction. J Am Coll Cardiol 2018;71(3):263–75.
65. Vera JH, Guo Q, Cole JH, et al. Neuroinflammation in treated HIV-positive individuals: a TSPO PET study. Neurology 2016;86(15):1425–32.
66. Muller C. Folate based radiopharmaceuticals for imaging and therapy of cancer and inflammation. Curr Pharm Des 2012;18(8):1058–83.
67. Salazar MD, Ratnam M. The folate receptor: what does it promise in tissue-targeted therapeutics? Cancer Metastasis Rev 2007;26(1):141–52.
68. Gent YY, Weijers K, Molthoff CF, et al. Evaluation of the novel folate receptor ligand [^{18}F]fluoro-PEG-folate for macrophage targeting in a rat model of arthritis. Arthritis Res Ther 2013;15(2):R37.
69. Xia W, Hilgenbrink AR, Matteson EL, et al. A functional folate receptor is induced during macrophage activation and can be used to target drugs to activated macrophages. Blood 2009;113(2):438–46.
70. Chandrupatla D, Molthoff CFM, Lammertsma AA, et al. The folate receptor beta as a macrophage-mediated imaging and therapeutic target in rheumatoid arthritis. Drug Deliv Transl Res 2019;9(1):366–78.
71. Hu Y, Wang B, Shen J, et al. Depletion of activated macrophages with a folate receptor-beta-specific

antibody improves symptoms in mouse models of rheumatoid arthritis. Arthritis Res Ther 2019;21(1):143.
72. Martinez-Pomares L. The mannose receptor. J Leukoc Biol 2012;92(6):1177–86.
73. Tahara N, Mukherjee J, de Haas HJ, et al. 2-Deoxy-2-[^{18}F]fluoro-D-mannose positron emission tomography imaging in atherosclerosis. Nat Med 2014;20(2):215–9.
74. Lee SP, Im HJ, Kang S, et al. Noninvasive imaging of myocardial inflammation in myocarditis using (68)Ga-tagged mannosylated human serum albumin positron emission tomography. Theranostics 2017;7(2):413–24.
75. Kim EJ, Kim S, Seo HS, et al. Novel PET imaging of atherosclerosis with ^{68}Ga-labeled NOTA-neomannosylated human serum albumin. J Nucl Med 2016;57(11):1792–7.
76. Varasteh Z, Mohanta S, Li Y, et al. Targeting mannose receptor expression on macrophages in atherosclerotic plaques of apolipoprotein E-knockout mice using (68)Ga-NOTA-anti-MMR nanobody: non-invasive imaging of atherosclerotic plaques. EJNMMI Res 2019;9(1):5.
77. Diaz LA Jr, Foss CA, Thornton K, et al. Imaging of musculoskeletal bacterial infections by [^{124}I]FIAU-PET/CT. PLoS One 2007;2(10):e1007.
78. Zhang XM, Zhang HH, McLeroth P, et al. [(124)I] FIAU: human dosimetry and infection imaging in patients with suspected prosthetic joint infection. Nucl Med Biol 2016;43(5):273–9.
79. Ning X, Seo W, Lee S, et al. PET imaging of bacterial infections with fluorine-18-labeled maltohexaose. Angew Chem Int Ed Engl 2014;53(51):14096–101.
80. Takemiya K, Ning X, Seo W, et al. Novel PET and near infrared imaging probes for the specific detection of bacterial infections associated with cardiac devices. JACC Cardiovasc Imaging 2019;12(5):875–86.
81. Lee HJ, Ehlerding EB, Cai W. Antibody-based tracers for PET/SPECT imaging of chronic inflammatory diseases. Chembiochem 2019;20(4):422–36.
82. Auletta S, Varani M, Horvat R, et al. PET radiopharmaceuticals for specific bacteria imaging: a systematic review. J Clin Med 2019;8(2) [pii:E197].
83. Herholz K, Holzer T, Bauer B, et al. ^{11}C-Methionine PET for differential diagnosis of low-grade gliomas. Neurology 1998;50(5):1316–22.
84. Kracht LW, Miletic H, Busch S, et al. Delineation of brain tumor extent with [11C]L-methionine positron emission tomography: local comparison with stereotactic histopathology. Clin Cancer Res 2004;10(21):7163–70.
85. Lapa C, Garcia-Velloso MJ, Luckerath K, et al. 11)C-Methionine-PET in multiple myeloma: a combined study from two different institutions. Theranostics 2017;7(11):2956–64.
86. Luckerath K, Lapa C, Albert C, et al. ^{11}C-Methionine-PET: a novel and sensitive tool for monitoring of early response to treatment in multiple myeloma. Oncotarget 2015;6(10):8418–29.
87. Luckerath K, Lapa C, Spahmann A, et al. Targeting paraprotein biosynthesis for non-invasive characterization of myeloma biology. PLoS One 2013;8(12):e84840.
88. Swirski FK, Nahrendorf M. Leukocyte behavior in atherosclerosis, myocardial infarction, and heart failure. Science 2013;339(6116):161–6.
89. Nahrendorf M. Myeloid cell contributions to cardiovascular health and disease. Nat Med 2018;24(6):711–20.
90. Oka S, Okudaira H, Ono M, et al. Differences in transport mechanisms of trans-1-amino-3-[^{18}F]fluorocyclobutanecarboxylic acid in inflammation, prostate cancer, and glioma cells: comparison with L-[methyl-^{11}C]methionine and 2-deoxy-2-[^{18}F]fluoro-D-glucose. Mol Imaging Biol 2014;16(3):322–9.
91. Morooka M, Kubota K, Kadowaki H, et al. ^{11}C-Methionine PET of acute myocardial infarction. J Nucl Med 2009;50(8):1283–7.
92. Thackeray JT, Bankstahl JP, Wang Y, et al. Targeting amino acid metabolism for molecular imaging of inflammation early after myocardial infarction. Theranostics 2016;6(11):1768–79.
93. Maya Y, Werner RA, Schutz C, et al. ^{11}C-Methionine PET of myocardial inflammation in a rat model of experimental autoimmune myocarditis. J Nucl Med 2016;57(12):1985–90.
94. Herrmann K, Buck AK. Proliferation imaging with (1)(8)F-fluorothymidine PET/computed tomography: physiologic uptake, variants, and pitfalls. PET Clin 2014;9(3):331–8.
95. Fuchs K, Kohlhofer U, Quintanilla-Martinez L, et al. In vivo imaging of cell proliferation enables the detection of the extent of experimental rheumatoid arthritis by 3'-deoxy-3'-^{18}F-fluorothymidine and small-animal PET. J Nucl Med 2013;54(1):151–8.
96. Norikane T, Yamamoto Y, Maeda Y, et al. Comparative evaluation of (18)F-FLT and (18)F-FDG for detecting cardiac and extra-cardiac thoracic involvement in patients with newly diagnosed sarcoidosis. EJNMMI Res 2017;7(1):69.
97. Martineau P, Pelletier-Galarneau M, Juneau D, et al. Imaging cardiac sarcoidosis with FLT-PET with comparison to FDG-PET: a prospective pilot study. J Nucl Med 2019;60(Suppl 1):670.
98. Blau M, Nagler W, Bender MA. Fluorine-18: a new isotope for bone scanning. J Nucl Med 1962;3:332–4.
99. Irmler IM, Gebhardt P, Hoffmann B, et al. ^{18}F-Fluoride positron emission tomography/computed tomography

for noninvasive in vivo quantification of pathophysiological bone metabolism in experimental murine arthritis. Arthritis Res Ther 2014;16(4):R155.
100. Watanabe T, Takase-Minegishi K, Ihata A, et al. 18) F-FDG and (18)F-NaF PET/CT demonstrate coupling of inflammation and accelerated bone turnover in rheumatoid arthritis. Mod Rheumatol 2016;26(2):180–7.
101. Derlin T, Wisotzki C, Richter U, et al. In vivo imaging of mineral deposition in carotid plaque using ^{18}F-sodium fluoride PET/CT: correlation with atherogenic risk factors. J Nucl Med 2011;52(3):362–8.
102. Derlin T, Richter U, Bannas P, et al. Feasibility of ^{18}F-sodium fluoride PET/CT for imaging of atherosclerotic plaque. J Nucl Med 2010;51(6):862–5.
103. Li Y, Berenji GR, Shaba WF, et al. Association of vascular fluoride uptake with vascular calcification and coronary artery disease. Nucl Med Commun 2012;33(1):14–20.
104. Dweck MR, Chow MW, Joshi NV, et al. Coronary arterial ^{18}F-sodium fluoride uptake: a novel marker of plaque biology. J Am Coll Cardiol 2012;59(17):1539–48.
105. Silva Mendes BI, Oliveira-Santos M, Vidigal Ferreira MJ. Sodium fluoride in cardiovascular disorders: a systematic review. J Nucl Cardiol 2019. https://doi.org/10.1007/s12350-019-01832-7.
106. McKenney-Drake ML, Moghbel MC, Paydary K, et al. (18)F-NaF and (18)F-FDG as molecular probes in the evaluation of atherosclerosis. Eur J Nucl Med Mol Imaging 2018;45(12):2190–200.
107. Vesey AT, Jenkins WS, Irkle A, et al. (18)F-Fluoride and (18)F-fluorodeoxyglucose positron emission tomography after transient ischemic attack or minor ischemic stroke: case-control study. Circ Cardiovasc Imaging 2017;10(3) [pii:e004976].
108. Blomberg BA, de Jong PA, Thomassen A, et al. Thoracic aorta calcification but not inflammation is associated with increased cardiovascular disease risk: results of the CAMONA study. Eur J Nucl Med Mol Imaging 2017;44(2):249–58.
109. Chowdhury MM, Tarkin JM, Albaghdadi MS, et al. Vascular positron emission tomography and restenosis in symptomatic peripheral arterial disease: a prospective clinical study. JACC Cardiovasc Imaging 2019. https://doi.org/10.1016/j.jcmg.2019.03.031.
110. Weinberg RL, Morgenstern R, DeLuca A, et al. F-18 sodium fluoride PET/CT does not effectively image myocardial inflammation due to suspected cardiac sarcoidosis. J Nucl Cardiol 2017;24(6):2015–8.
111. Moisio O, Siitonen R, Liljenback H, et al. Exploring alternative radiolabeling strategies for sialic acid-binding immunoglobulin-like lectin 9 peptide: [(68)Ga]Ga- and [(18)F]AlF-NOTA-Siglec-9. Molecules 2018;23(2) [pii:E305].
112. Lankinen P, Makinen TJ, Poyhonen TA, et al. (68) Ga-DOTAVAP-P1 PET imaging capable of demonstrating the phase of inflammation in healing bones and the progress of infection in osteomyelitic bones. Eur J Nucl Med Mol Imaging 2008;35(2):352–64.
113. Autio A, Vainio PJ, Suilamo S, et al. Preclinical evaluation of a radioiodinated fully human antibody for in vivo imaging of vascular adhesion protein-1-positive vasculature in inflammation. J Nucl Med 2013;54(8):1315–9.
114. Autio A, Henttinen T, Sipila HJ, et al. Mini-PEG spaceing of VAP-1-targeting 68Ga-DOTAVAP-P1 peptide improves PET imaging of inflammation. EJNMMI Res 2011;1(1):10.
115. Aalto K, Autio A, Kiss EA, et al. Siglec-9 is a novel leukocyte ligand for vascular adhesion protein-1 and can be used in PET imaging of inflammation and cancer. Blood 2011;118(13):3725–33.
116. McMurray RW. Adhesion molecules in autoimmune disease. Semin Arthritis Rheum 1996;25(4):215–33.
117. Ley K. The role of selectins in inflammation and disease. Trends Mol Med 2003;9(6):263–8.
118. Li X, Bauer W, Israel I, et al. Targeting P-selectin by gallium-68-labeled fucoidan positron emission tomography for noninvasive characterization of vulnerable plaques: correlation with in vivo 17.6T MRI. Arterioscler Thromb Vasc Biol 2014;34(8):1661–7.
119. Nakamura I, Hasegawa K, Wada Y, et al. Detection of early stage atherosclerotic plaques using PET and CT fusion imaging targeting P-selectin in low density lipoprotein receptor-deficient mice. Biochem Biophys Res Commun 2013;433(1):47–51.
120. Xu Y, Li J, Fang W, et al. A potential thrombus diagnosis reagent based on P-selectin monoclonal antibody SZ-51 light chain. Thromb Res 2008;123(2):306–15.
121. Kolb HC, Barret O, Bhattacharya A, et al. Preclinical evaluation and nonhuman primate receptor occupancy study of (18)F-JNJ-64413739, a PET radioligand for P2X7 receptors. J Nucl Med 2019;60(8):1154–9.
122. Territo PR, Meyer JA, Peters JS, et al. Characterization of (11)C-GSK1482160 for targeting the P2X7 receptor as a biomarker for neuroinflammation. J Nucl Med 2017;58(3):458–65.
123. Ory D, Celen S, Gijsbers R, et al. Preclinical evaluation of a P2X7 receptor-selective radiotracer: PET studies in a rat model with local overexpression of the human P2X7 receptor and in nonhuman primates. J Nucl Med 2016;57(9):1436–41.
124. Fantoni ER, Dal Ben D, Falzoni S, et al. Design, synthesis and evaluation in an LPS rodent model of neuroinflammation of a novel (18)F-labelled PET tracer targeting P2X7. EJNMMI Res 2017;7(1):31.

125. Jin H, Han J, Resing D, et al. Synthesis and in vitro characterization of a P2X7 radioligand [(123)I] TZ6019 and its response to neuroinflammation in a mouse model of Alzheimer disease. Eur J Pharmacol 2018;820:8–17.
126. Janssen B, Vugts DJ, Wilkinson SM, et al. Identification of the allosteric P2X7 receptor antagonist [(11)C]SMW139 as a PET tracer of microglial activation. Sci Rep 2018;8(1):6580.
127. Fu Z, Lin Q, Hu B, et al. P2X7 PET radioligand (18) F-PTTP for differentiation of lung tumor from inflammation. J Nucl Med 2019;60(7):930–6.
128. Hamson EJ, Keane FM, Tholen S, et al. Understanding fibroblast activation protein (FAP): substrates, activities, expression and targeting for cancer therapy. Proteomics Clin Appl 2014;8(5–6):454–63.
129. Welt S, Divgi CR, Scott AM, et al. Antibody targeting in metastatic colon cancer: a phase I study of monoclonal antibody F19 against a cell-surface protein of reactive tumor stromal fibroblasts. J Clin Oncol 1994;12(6):1193–203.
130. Terry SY, Koenders MI, Franssen GM, et al. Monitoring therapy response of experimental arthritis with radiolabeled tracers targeting fibroblasts, macrophages, or integrin alphavbeta3. J Nucl Med 2016;57(3):467–72.
131. Laverman P, van der Geest T, Terry SY, et al. Immuno-PET and immuno-SPECT of rheumatoid arthritis with radiolabeled anti-fibroblast activation protein antibody correlates with severity of arthritis. J Nucl Med 2015;56(5):778–83.
132. van der Geest T, Laverman P, Gerrits D, et al. Liposomal treatment of experimental arthritis can be monitored noninvasively with a radiolabeled anti-fibroblast activation protein antibody. J Nucl Med 2017;58(1):151–5.
133. Loktev A, Lindner T, Mier W, et al. A tumor-imaging method targeting cancer-associated fibroblasts. J Nucl Med 2018;59(9):1423–9.
134. Lindner T, Loktev A, Altmann A, et al. Development of quinoline-based theranostic ligands for the targeting of fibroblast activation protein. J Nucl Med 2018;59(9):1415–22.
135. Majmudar MD, Yoo J, Keliher EJ, et al. Polymeric nanoparticle PET/MR imaging allows macrophage detection in atherosclerotic plaques. Circ Res 2013;112(5):755–61.
136. Keliher EJ, Ye YX, Wojtkiewicz GR, et al. Polyglucose nanoparticles with renal elimination and macrophage avidity facilitate PET imaging in ischaemic heart disease. Nat Commun 2017;8:14064.
137. Kouijzer IJE, Mulders-Manders CM, Bleeker-Rovers CP, et al. Fever of unknown origin: the value of FDG-PET/CT. Semin Nucl Med 2018;48(2):100–7.
138. Mahmood M, Kendi AT, Ajmal S, et al. Meta-analysis of 18F-FDG PET/CT in the diagnosis of infective endocarditis. J Nucl Cardiol 2019;26(3):922–35.
139. Piekarski E, Benali K, Rouzet F. Nuclear imaging in sarcoidosis. Semin Nucl Med 2018;48(3):246–60.
140. Matter CM, Wyss MT, Meier P, et al. ^{18}F-Choline images murine atherosclerotic plaques ex vivo. Arterioscler Thromb Vasc Biol 2006;26(3):584–9.
141. Blockmans D, de Ceuninck L, Vanderschueren S, et al. Repetitive ^{18}F-fluorodeoxyglucose positron emission tomography in giant cell arteritis: a prospective study of 35 patients. Arthritis Rheum 2006;55(1):131–7.
142. Yamashita H, Kubota K, Mimori A. Clinical value of whole-body PET/CT in patients with active rheumatic diseases. Arthritis Res Ther 2014;16(5):423.
143. Ramirez R, Trivieri M, Fayad ZA, et al. Advanced imaging in cardiac sarcoidosis. J Nucl Med 2019;60(7):892–8.